Autocorrelation Measurement of Fast Electron Pulses Emitted through the Interaction of Femtosecond Laser Pulses with a Solid Target

Shunsuke Inoue,[1,2,*] Shigeki Tokita,[1,2] Kazuto Otani,[1,2] Masaki Hashida,[1,2] Masayasu Hata,[3] Hitoshi Sakagami,[4] Toshihiro Taguchi,[5] and Shuji Sakabe[1,2]

[1]*Advanced Research Center for Beam Science, Institute for Chemical Research, Kyoto University, Gokasho, Uji, Kyoto 611-0011, Japan*

[2]*Department of Physics, Graduate School of Science, Kyoto University, Kitashirakawa, Sakyo, Kyoto 606-8502, Japan*

[3]*Department of Physics, Nagoya University, Nagoya, Aichi 464-8602, Japan*

[4]*Fundamental Physics Simulation Division, National Institute for Fusion Science, Toki, Gifu 509-5292, Japan*

[5]*Department of Electrical and Electronic Engineering, Setsunan University, Neyagawa, Osaka 572-8508, Japan*

(Received 15 May 2012; published 31 October 2012)

We report the first direct measurement of the emission duration of laser-accelerated fast electrons from the surface of a solid target irradiated by a high-intensity femtosecond laser pulse. The emission duration is determined by autocorrelation measurement using the Coulomb repulsive forces that act on two equivalent electron pulses. The emission duration depends on the laser pulse duration for laser pulses of 200–690 fs. Numerical modeling of three-dimensional charged particle dynamics indicates that the emission duration of fast electrons is almost equal to the duration of the laser pulse.

DOI: 10.1103/PhysRevLett.109.185001 PACS numbers: 52.38.Kd, 06.60.Jn, 52.70.Nc

The interactions of intense short-pulse lasers with solid targets accelerate electrons to high energy and relativistic speed, and the resulting fast electrons induce intense emissions of ions [1,2], x rays [3,4], gamma rays [5], and terahertz waves [6,7]. The generation dynamics and characteristics of such emissions are deeply related to the temporal and spatial characteristics of fast electrons during or immediately after the laser pulse. Therefore, understanding the initial dynamics of fast electrons is an important open issue for developing many attractive applications such as fast ignition for inertial confinement fusion [8,9], tumor therapy using ion beams [10], ultrafast electron diffraction measurement [11,12], and time-resolved x-ray probing [13,14].

Currently, the prevailing theory is that an intense laser pulse strongly interacts with plasma around the critical density, and the energy of the incident laser pulse is partially transferred to the fast electrons [15–17]. Extensive numerical simulations and experimental studies indicate that the fast electrons are accelerated during the laser pulse. Observing the temporal structure of fast electrons, however, remains a challenging problem because they are accelerated and emitted on an ultrafast time scale, typically from femtoseconds to picoseconds. For elucidating fast electron dynamics, the temporal resolution of diagnostics has been improved through various techniques. For example, time-resolved measurement of K_α radiation induced by fast electrons has been achieved with an ultrafast x-ray streak camera [18,19]. Those experiments reveal the hot-electron dynamics in solid targets at picosecond temporal resolution. The pulse duration of K_α radiation have been investigated through ultrafast phenomena and measured to be several times larger than the laser pulse duration, corresponding to a few or several hundred femtoseconds [20,21]. These measurements indicated that the electron pulse duration is shorter than the K_α x-ray pulse duration. Radiography using laser-driven proton beams has been also applied in studying the dynamics of ultrafast electromagnetic fields [22,23]. The temporal resolution of proton radiography measurement depends on the pulse duration of the laser-accelerated proton beam and is constrained to a few picoseconds. For higher temporal resolution, interferometric measurement of electron distributions has been performed by using optical probe pulses [24]. The temporal evolution of the electron sheath around the solid target has been observed at 200 fs intervals, but in optical interferometry, the detectable range of the electron density is limited. Hence, there is no adequate real-time measurement technique for observing the detailed temporal structure of fast electrons, and the response of the fast electrons to the incident laser pulse is still not completely understood.

To investigate the femtosecond-scale dynamics of fast electrons, we have developed a femtosecond electron deflectometry method [25]. In this method, by employing a laser-accelerated electron pulse as a probe pulse, we have measured the dynamics of the fast-electron-induced electric field, which varies within 400 fs after the laser pulse irradiation on a solid target. In this Letter, we describe autocorrelation measurement using two equivalent fast electron pulses for determining the duration of fast electron emission from the surface of a solid target. The obtained data show that the emission duration clearly depends on laser pulse duration on a femtosecond time scale of about 200–690 fs. Numerical modeling of electron dynamics in the experimental configuration reveals that the emission

duration of fast electrons is almost equal to the duration of the laser pulse.

The experimental setup for the autocorrelation measurement is schematically shown in Fig. 1. The experiments were performed using a Ti:sapphire chirped-pulse amplification (CPA) system (center wavelength, 800 nm; repetition rate, 10 Hz). A laser pulse is divided into half-pulses of equal energy (upper pulse and lower pulse in Fig. 1), and the half-pulses are focused onto a solid target (Al foil, 12 μm thick) with p-polarization at an incident angle of 45° by using an $F/3$ off-axis parabolic mirror. The distance between the two focal positions for the upper and lower laser pulses is adjusted to 27 ± 1 μm. The lower laser pulse propagates through an optical delay line, and the time delay (τ) between the upper and lower pulses is varied from -2.6 to 2.6 ps at time steps of 65 fs. The zero delay time can be determined by observing the interference fringe of the upper and lower pulses at a defocused position without a target. The position of the target surface is carefully measured with a laser displacement sensor and precisely adjusted, so that the displacements of the target surface from the laser focal positions are less than ± 1.2 μm in standard deviation. The laser pulse duration is set at 200, 410, 540, or 690 fs full width at half-maximum (FWHM) by controlling the distance between the pair of gratings that constitute the pulse compressor of the CPA laser system. The laser pulse energy is controlled in order that the intensity of each pulse on the target is 1×10^{16} W/cm^2. The laser-intensity contrast is about 10^{-7} at 20 ps before the peak of the main laser pulse.

The two laser pulses produce two equivalent electron pulses. The angular distribution of these electrons for each

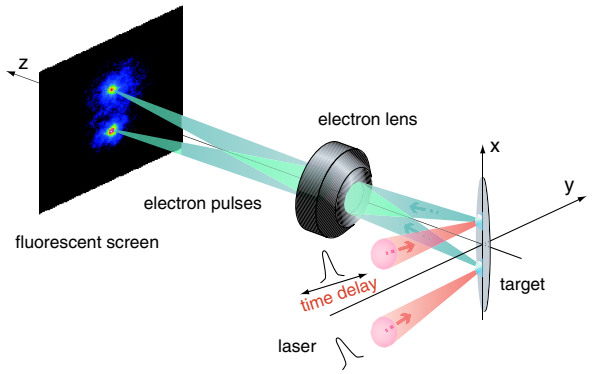

FIG. 1 (color online). Schematic of the experimental setup. Two equivalent laser pulses with a time delay between them are focused on an Al target to produce two electron pulses. The time delay between them is variable from -2.6 to 2.6 ps in time steps of 65 fs. The laser-accelerated electrons are emitted isotropically. A selected portion of the electrons that pass through the electron lens can be focused on a fluorescent screen. The electron pulses are deflected by each of the laser plasmas immediately after they are emitted from the target; consequently, the distance between the source image positions on the fluorescent screen depends on the time delay.

laser pulse duration is measured separately by imaging plates, and the electrons are emitted omnidirectionally. The electrons emitted in the specular direction from the two irradiated positions are collected and focused onto a fluorescent screen by an electron lens. The sensitivity of the present imaging system is high enough for the electron source image to be obtained by a single laser shot [26]. The energy spectrum of electrons emitted in the specular direction is also separately measured for each pulse duration by a magnetic spectrometer with an imaging plate, and can be fitted to the Boltzmann distribution with a temperature of about 60 keV. The energy of electrons imaged on the screen is selected to be 120 keV by the electron lens [26].

When the time delay between the upper and lower laser pulses is small, the two electron pulses will be deflected by the Coulomb repulsive force between them, immediately after they are emitted from the target. This deflection is observed as a shortened distance between the two electron source positions imaged on the screen [25]. If the two electron pulses are equivalent, the deflection as a function of time delay can be treated as an autocorrelation of the time-varying intensity of electrons emitted from the target surface. However, the distance between the two laser irradiation positions on the target is short in our experimental setup. Laser pulse irradiation at one position heats the target and generates electric or magnetic fields on the target surface, and thus we must consider whether there is an influence on the electron emission duration at the other position. To confirm the equivalence of each electron emission, we carried out numerical simulations using the 2D particle-in-cell code FISCOF2 [27]. In the simulations, p-polarized laser pulses are irradiated onto a planar plasma at an incidence of 45°. At the surface, the density of the plasma increases exponentially from $0.1n_c$ to $4.0n_c$ over 2.7 μm and remains constant at $4.0n_c$ over 5 μm, where $n_c = 1.7 \times 10^{21}$ cm^{-3}. The initial electron and ion (Al^+) temperatures are 0.1 keV and 3 eV, respectively. The spatial and temporal distributions of the incident laser pulses are Gaussian, and the pulse durations and spot sizes are fixed at 200 fs and 5 μm (FWHM), corresponding to intensity of 1×10^{16} W/cm^2. First, we simulated a single laser pulse. At the laser irradiation position, the electron temperature increases to 3 keV. At 27 μm away from the laser irradiation position on the target and 1 ps after laser pulse irradiation, the electron density does not change and the electron temperature slightly increases (0.2 keV). Although a static electric field is produced on the target surface by the laser irradiation, the maximum intensity at the position 27 μm away from the laser irradiation position is 24 times lower (1.9×10^{10} V/m) than that at the laser irradiation position. Then, we simulated two laser pulses. The second laser pulse is irradiated at a time delay of 200 or 400 fs after the first laser pulse. The distance between the irradiation positions of the two laser pulses is 27 μm. We find no difference in electron density, electron

temperature, or static electric field intensity at the irradiation position of the second (delayed) pulse between the cases with and without the first laser pulse. Therefore, we conclude that the interaction between the two electron sources is sufficiently small for the two electron pulses to be considered equivalent.

The autocorrelation measurement of the emission duration of electron pulses for laser pulses of 200, 410, 540, and 690 fs are shown in Fig. 2(a) as circles. The deflection is normalized by each maximum value and the time delay is between the two incident laser pulses. The maximum deflection in Fig. 2(a) is about 10 μm in objective space. Each point is obtained by averaging 30–50 deflection data, and the error bars indicate the standard deviation. For any laser pulse duration, the deflection decreases when the time delay between the laser pulses is increased. When the magnitude of the time delay is greater than 1.5 ps, no deflection is observed, meaning that a detectable electromagnetic field exists for time delays of only -1.5 to 1.5 ps. As we have shown previously [25], the Coulomb repulsive force from a fast electron pulse is dominant on this time scale. Figure 2(b) shows the dependence of the interaction time of the two electron pulses on the laser pulse duration. The interaction time is defined as the temporal duration (FWHM) of the autocorrelation measurement result shown in Fig. 2(a). The figure shows that the interaction time of the electron pulses increases as the laser pulse duration is increased. The emission duration of the electron pulses from the target surface closely correlates with laser pulse duration on the femtosecond time scale.

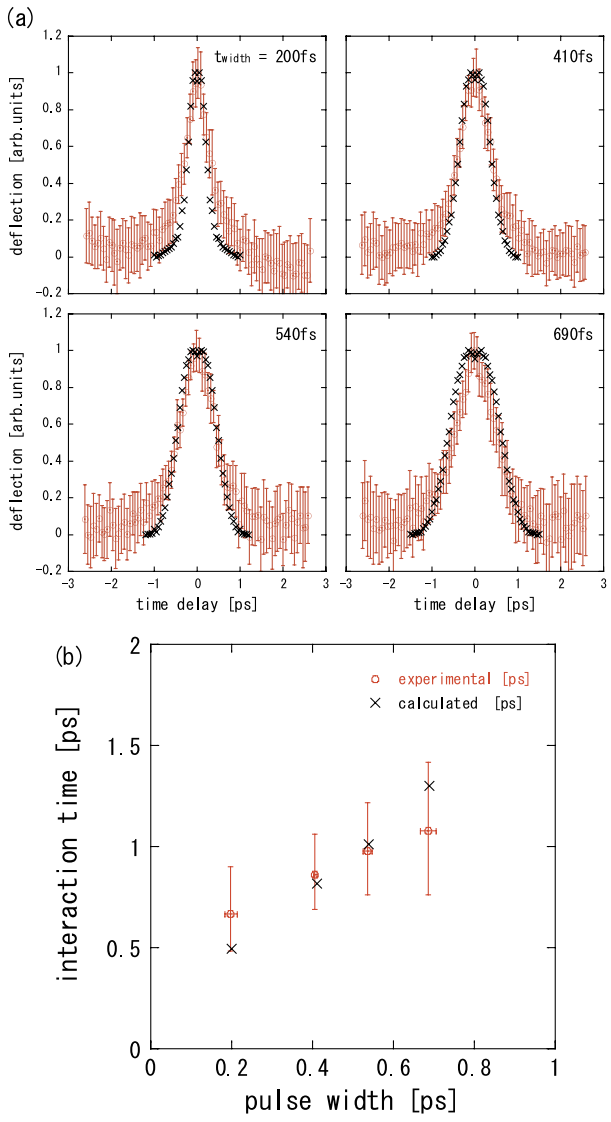

FIG. 2 (color online). (a) Deflections of electron pulses as a function of time delay for laser pulse durations (t_{width}) of 200, 410, 540, and 690 fs (circle). Each point is obtained by averaging 30-50 data points, and error bars indicate standard deviation. The deflection is normalized by each maximum value. Deflections calculated with the GPT code are shown as crosses. (b) Interaction time of the electron pulses obtained from experiments (circle) and numerical calculations (cross) as a function of laser pulse duration and initial electron pulse duration, respectively. The error bars show the fitting error for the autocorrelation traces in (a).

To estimate the pulse duration of fast electrons from the autocorrelation trace, we reconstruct the autocorrelation function through numerical calculations. The autocorrelation function can be reconstructed by calculating the Lorentz force that the two fast electron pulses produce, if the deflection is caused by their induced electromagnetic fields. By making an assumption about the temporal shape of the electron pulses produced by the incident laser pulses, the autocorrelation function can be obtained. By comparing the measured and calculated autocorrelation function, we can thus estimate the electron pulse durations.

To simulate the electromagnetic fields produced by electron pulses, we used the GENERAL PARTICLE TRACER (GPT) code [28], which can calculate the electromagnetic fields produced by charged particles (space charge field). In the simulation, two electron pulses produced at the laser focal spots are initially separated from each other by 27 μm in free space. The effect of the boundary condition at the metal interface is not taken into account in the present simulation. The time delay between two electron pulses is varied at intervals of 50 fs. The initial electron pulses are assumed to be emitted from $z = 0$ into the hemisphere, of which the zenith is on the z axis, with isotropic angular distribution. The coordinates are the same as those shown in Fig. 1. The electrons injected into $z < -10$ μm because of the Lorentz force are excluded. The initial temperature and total charge of one electron pulse are 60 keV and 0.3 nC, respectively. These initial conditions of the electron pulses are based on our experimental results. The temporal distribution of an electron pulse is assumed to be a Gaussian function, and the electron pulse duration is assumed to be 200, 410, 540, or 690 fs FWHM, corresponding to the laser pulse durations. Figure 3 shows an example of calculated

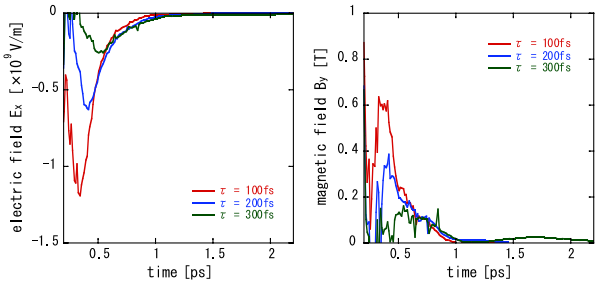

FIG. 3 (color online). Time course of electric and magnetic fields that act on an electron pulses with different time delay τ for electron pulse duration of 200 fs. Electric field is along the y axis in Fig. 1; magnetic field, the x axis.

electromagnetic fields produced by the electron pulses for various time delays. The electron pulse width is assumed to be 200 fs, and the central time of an electron pulse is assumed to be $200 + \tau$ fs. Lines indicate the time course of electric field along the x axis and magnetic field along the y axis. The electromagnetic fields shown in Fig. 3 are those of the delayed electron pulse. From these calculated electromagnetic fields, the deflection $d(\tau)$ is given by [25]

$$d(\tau) = -\frac{e}{m_e \gamma} \iint_{\tau} dt^2 [E_x(t) + c\beta B_y(t)],$$

where $E_x(t)$ is the electric field along the x direction and $B_y(t)$ is the magnetic field along the y direction (the axes are shown in Fig. 1), e is the elementary charge, and m_e is the electron mass. In our experiments, the observed kinetic energy of electron pulses is 120 keV, and thus we take account of relativistic effects: γ is the Lorentz factor and β is the ratio of electron velocity to the speed of light c. The calculated deflections for the present electron pulse durations are shown in Fig. 2 as crosses. The shapes of autocorrelation functions measured from experimental results are fairly in good agreement with that calculated from the numerical results, when the laser pulse duration is assumed to be as short as the electron pulse duration [Fig. 2(a)]. In the present model, the autocorrelation function is reproducible when taking into account only the electromagnetic fields produced by electron pulses in free space. This suggests that the autocorrelation measurement of the electron pulses is not strongly influenced by environmental factors such as the target or laser-produced plasma under the present experimental conditions. The calculated interaction time is also shown in Fig. 2(b). The increase in the interaction time is reproduced in the numerical results. This indicates that electrons are accelerated and emitted only while the laser pulse interacts with the target surface and that the pulse duration of the fast electrons is almost equal to the laser pulse duration.

In conclusion, the temporal structures of fast electrons emitted immediately after irradiation of the surface of a solid target by an intense femtosecond laser pulse have been studied through autocorrelation measurement of the fast electron pulses. Time-resolved measurement of the electric field produced by fast electrons shows that the emission duration of the emitted fast electrons depended on laser pulse duration on the femtosecond scale, for pulses of 200, 410, 540, and 690 fs. We note that changing the pulse duration by roughly 100 fs resulted in a remarkable change in the emission duration of fast electrons. Numerical modeling of electron dynamics indicated that the emission duration of fast electrons is almost equal to the laser pulse duration. These experiments were carried out using a laser intensity of 1×10^{16} W/cm^2, but this technique essentially can be applied in research on higher intensity laser-plasma interactions. This work contributes to the understanding of laser-plasma physics and the development of advanced radiation applications based on ultrafast electron dynamics.

This work was supported by a Grant-in-Aid for Challenging Exploratory Research (Grant No. 22654050), a Grant-in-Aid for Scientific Research (S) (Grant No. 23226002), a Grant-in-Aid for Scientific Research (C) (Grant No. 24540537), Yamada Science Foundation, Mitsubishi Foundation, and a Grant-in-Aid for the Global COE Program "The Next Generation of Physics, Spun from Universality and Emergence" from the Ministry of Education, Culture, Sports, Science and Technology (MEXT) of Japan. S. I. is supported by a Grant-in-Aid from the Japan Society for Promotion of Science (JSPS).

*Corresponding author.

[1] S. C. Wilks, A. B. Langdon, T. E. Cowan, M. Roth, M. Singh, S. Hatchett, M. H. Key, D. Pennington, A. MacKinnon, and R. A. Snavely, Phys. Plasmas **8**, 542 (2001).

[2] M. Roth, A. Blazevic, M. Geissel, T. Schlegel, T. E. Cowan, M. Allen, J.-C. Gauthier, P. Audebert, J. Fuchs, J. Meyer-ter-Vehn, M. Hegelich, S. Karsch, and A. Pukhov, Phys. Rev. ST Accel. Beams **5**, 061301 (2002).

[3] J. D. Kmetec, C. L. Gordon, J. J. Macklin, B. E. Lemoff, G. S. Brown, and S. E. Harris, Phys. Rev. Lett. **68**, 1527 (1992).

[4] Ch. Reich, P. Gibbon, I. Uschmann, and E. Förster, Phys. Rev. Lett. **84**, 4846 (2000).

[5] P. A. Norreys, M. Santala, E. Clark, M. Zepf, I. Watts, F. N. Beg, K. Krushelnick, M. Tatarakis, A. E. Dangor, X. Fang, P. Graham, T. McCanny, R. P. Singhal, K. W. D. Ledingham, A. Creswell, D. C. W. Sanderson, J. Magill, A. Machacek, J. S. Wark, R. Allott, B. Kennedy, and D. Neely, Phys. Plasmas **6**, 2150 (1999).

[6] H. Hamster, A. Sullivan, S. Gordon, W. White, and R. W. Falcone, Phys. Rev. Lett. **71**, 2725 (1993).

[7] Z. Jin, Z. L. Chen, H. B. Zhuo, A. Kon, M. Nakatsutsumi, H. B. Wang, B. H. Zhang, Y. Q. Gu, Y. C. Wu, B. Zhu, L. Wang, M. Y. Yu, Z. M. Sheng, and R. Kodama, Phys. Rev. Lett. **107**, 265003 (2011).

[8] M. Tabak, J. Hammer, M. E. Glinsky, W. L. Kruer, S. C. Wilks, J. Woodworth, E. M. Campbell, M. D. Perry, and R. J. Mason, Phys. Plasmas **1**, 1626 (1994).
[9] S. Atzeni, Phys. Plasmas **6**, 3316 (1999).
[10] S. V. Bulanov and V. S. Khoroshkov, Plasma Phys. Rep. **28**, 453 (2002).
[11] S. Tokita, S. Inoue, S. Masuno, M. Hashida, and S. Sakabe, Appl. Phys. Lett. **95**, 111911 (2009).
[12] S. Tokita, M. Hashida, S. Inoue, T. Nishoji, K. Otani, and S. Sakabe, Phys. Rev. Lett. **105**, 215004 (2010).
[13] A. Rousse, C. Rischel, S. Fourmaux, I. Uschmann, S. Sebban, G. Grillon, Ph. Balcou, E. Förster, J. P. Geindre, P. Audebert, J. C. Gauthier, and D. Hulin, Nature (London) **410**, 65 (2001).
[14] C. W. Siders, A. Cavalleri, K. Sokolowski-Tinten, Cs. Tóth, T. Guo, M. Kammler, M. Horn von Hoegen, K. R. Wilson, D. von der Linde, and C. P. J. Barty, Science **286**, 1340 (1999).
[15] W. L. Kruer, *The Physics of Laser Plasma Interactions* (Westview Press, Boulder, CO, 2003).
[16] F. Brunel, Phys. Rev. Lett. **59**, 52 (1987).
[17] W. L. Kruer and Kent Estabrook, Phys. Fluids **28**, 430 (1985).
[18] C. R. D. Brown, D. J. Hoarty, S. F. James, D. Swatton, S. J. Hughes, J. W. Morton, T. M. Guymer, M. P. Hill, D. A. Chapman, J. E. Andrew, A. J. Comley, R. Shepherd, J. Dunn, H. Chen, M. Schneider, G. Brown, P. Beiersdorfer, and J. Emig, Phys. Rev. Lett. **106**, 185003 (2011).
[19] P. M. Nilson, J. R. Davies, W. Theobald, P. A. Jaanimagi, C. Mileham, R. K. Jungquist, C. Stoeckl, I. A. Begishev, A. A. Solodov, J. F. Myatt, J. D. Zuegel, T. C. Sangster, R. Betti, and D. D. Meyerhofer, Phys. Rev. Lett. **108**, 085002 (2012).
[20] T. Feurer, A. Morak, I. Uschmann, Ch. Ziener, H. Schwoerer, Ch. Reich, P. Gibbon, E. Forster, R. Sauerbrey, K. Ortner, and C. R. Becker, Phys. Rev. E **65**, 016412 (2001).
[21] K. Sokolowski-Tinten, C. Blome, C. Dietrich, A. Tarasevitch, M. Horn von Hoegen, D. von der Linde, A. Cavalleri, J. Squier, and M. Kammler, Phys. Rev. Lett. **87**, 225701 (2001).
[22] L. Romagnani, J. Fuchs, M. Borghesi, P. Antici, P. Audebert, F. Ceccherini, T. Cowan, T. Grismayer, S. Kar, A. Macchi, P. Mora, G. Pretzler, A. Schiavi, T. Toncian, and O. Willi, Phys. Rev. Lett. **95**, 195001 (2005).
[23] K. Quinn, P. A. Wilson, C. A. Cecchetti, B. Ramakrishna, L. Romagnani, G. Sarri, L. Lancia, J. Fuchs, A. Pipahl, T. Toncian, O. Willi, R. J. Clarke, D. Neely, M. Notley, P. Gallegos, D. C. Carroll, M. N. Quinn, X. H. Yuan, P. McKenna, T. V. Liseykina, A. Macchi, and M. Borghesi, Phys. Rev. Lett. **102**, 194801 (2009).
[24] O. Jäckel, J. Polz, S. M. Pfotenhauer, H.-P. Schlenvoigt, H. Schwoerer, and M. C. Kaluza, New J. Phys. **12**, 103027 (2010).
[25] Shunsuke Inoue, Shigeki Tokita, Kazuto Otani, Masaki Hashida, and Shuji Sakabe, Appl. Phys. Lett. **99**, 031501 (2011).
[26] Shunsuke Inoue, Shigeki Tokita, Toshihiko Nishoji, Shinichiro Masuno, Kazuto Otani, Masaki Hashida, and Shuji Sakabe, Rev. Sci. Instrum. **81**, 123302 (2010).
[27] H. Sakagami and K. Mima, *Proceedings of the 2nd International Conference on Inertial Fusion Science and Applications, Kyoto, 2001* (Elsevier, New York, 2002), p. 380.
[28] General Particle Tracer, http://www.pulsar.nl/gpt.